I.A.U
Karaj branch

Journal of
A p p l ied
C hemical
R esearch
jacr.kiau.ac.ir

Journal of Applied Chemical Research, 17, 2, 8-25 (2023)

The Use of Nanoemulsion-based Strategies to Improve Corrosion inhibition Efficiency of Herbal Extract Inhibitors

Meysam Ahmadi-Zeidabadi[1], Razieh Razavi[2*], Mahnaz Amiri[1,3*], Seyed Hamzeh Hosseini[4], Maryam Payandeh[4]

[1]Neuroscience Research Center, Institute of Neuropharmacology, Kerman University of Medical Science, Kerman, Iran

[2]Department of Chemistry, Faculty of Science, University of Jiroft, Jiroft, Iran

[3]Cell Therapy and Regenerative Medicine Comprehensive Center, Kerman University of Medical Science, Kerman, Iran

[4]Department of Biology, Faculty of Science, University of Jiroft, Jiroft, Iran

(Received 21 Aug. 2022; Final revision received 20 Nov. 2022)

Abstract

The requirement for abiding by strict environmental protection regulations has caused many researchers during the past decades to go after using green and cheap compounds available from renewable sources like plant metabolites (bioactive compounds). Improving the corrosion prevention effect of various plant extracts is of utmost importance in this regard, for which a novel nanoemulsion-based strategy is proposed in the present paper. The corrosion inhibitors that participated in this study included *Amaranthus*, *Althermanthea,* and *Cionura erecta* (*L*.) *Griseb*, which was investigated against mild steel in 0.5 mol·L^{-1} HCl media. The presented data were obtained via electrochemical techniques (EIS and polarization)and surface analyses (SEM). The researchers also used Dynamic light scattering to evaluate the particles' sizes in nanoemulsion solutions. Nanoemulsions indicated hydrodynamic diameter below 500 nm, meanwhile having narrow particle size distribution. Findings presented that 100 mg/L of Amaranthus extract nanoemulsion resulted in an inhibition efficiency of 91%, denoting that a slight amount of Amaranthus inhibitor extract could produce greater efficiency. The SEM analysis results were decisive in proving that the

absorption of Amaranthus molecules on the surface of metal decreased its dissolution rate substantially, producing a smooth and clean surface. One primary reason for the effective adsorption of extracts on metal surfaces via chelation with iron atoms refers to the presence of an abundant number of electron donor Oxygen- based atoms in the molecules of different aerial parts of the extracts. Further description for the extract inhibitory mechanism is the physical adsorption of the section on the surface layer of metal followed by the Langmuir adsorption isotherm. The nanoemulsion Amaranthus extract in this process absorbs approx. -24.7 kJ·mol−1 of free energy. the cytotoxicity test through MTT assay on A172 and SHSY5Y cell lines was used, revealing the therapeutic impact on initiating cytotoxic response in neural cell lines, and anticancer activity.

Keywords: Inhibitor, Green corrosion, Cell lines, Anticancer, Nanoemulsion, Herbal plants.

*__Corresponding authors:__ *Razieh Razavi, Department of Chemistry, Faculty of Science, University of Jiroft, Jiroft, Iran. Email: R.Razavi@ujiroft.ac.ir.*
Mahnaz Amiri, Neuroscience Research Center, Institute of Neuropharmacology, Kerman University of Medical Science, Kerman, Iran, Cell Therapy and Regenerative Medicine Comprehensive Center, Kerman University of Medical Science, Kerman, Iran.

Introduction

Pickling, modern cleaning, and descaling industry use various substances including acidic solutions in their treatment processes [1-3]. Metals and alloys are often vulnerable to corrosion phenomena that would increase the formation of thicker corroded films by direct reaction with the adjacent substances and environmental constituents [4]. Resulting in tremendous cost, and loss of energy and materials as well. Hence, an abundant number of studies have been undertaken to develop more efficient methods to counter corrosion and effectively protect the metals. To mitigate this problem, specifically in acidic environments, corrosion inhibitors ― commonly classified as inorganic and organic― are now an affordable and widely used, yet progressive solution approach [5, 6]. Due to the higher inhibition efficiency, they can yield [7].

Studies have shown that heteroatoms like nitrogen, oxygen, phosphorus and sulphur found in organic molecules, and multiple bonds and aromatic rings, are good metal corrosion inhibitors in acidic environments [8]. The drawback, however, is that many organic inhibitors are poisonous to the human body meanwhile producing adverse effects on the environment [9]. In response to the hazardous effects attributable to the organic inhibitors, the "Green chemistry" has been developing during the recent decade in the form of non-toxic green inhibitor compounds [10] like biopolymers [11] and ionic liquids [12-14], obtainable from inexpensive environmentally friendly resources.

It has been worth mentioning that different parts of plants and fruits, such as roots, leaves, shells, and seeds (or peels), have been previously utilized to mitigate the corrosion of metal surfaces [15]. The selection of a corrosion inhibitor for a specific application, several factors, including the inhibition efficiency, cost-effectiveness, accessibility, and environmental friendliness, should be taken into account. Hence, the use of natural products as anti-corrosive agents has been widely studied due to their non-toxicity, inexpensiveness, biodegradability, and ease of accessibility. Accordingly, numerous herbal extracts have been proposed as efficient corrosion inhibitors for steel in acidic spaces [16]. The extract of Sunflower seed hull [17], Hibiscus sabdariffa [18], Neem [19], Propolis [20], Pectin [21], Tagetes erecta [22], Henna [23], Musa paradisiaca peel [24], Lemon Balm [25], Mangifera indica (mango) leaves [26], Pyrazine derivatives [27], Glycyrrhiza glabra leaves [28], Cashew nut shell liquid [29] are some of the corrosion inhibitors, to name a few.

The presence of organic compounds such as tannins, alkaloids, carbohydrates, and amino acids containing polar groups such as N, S, and O atoms is the major cause of the inhibitory function of plant extracts. Also, the existence of double bonds and aromatic rings are crucial

as adsorbent sites. Amaranthus cordatus as a Green Corrosion Inhibitor for Mild Steel in H2SO4 and NaCl. There are not any reports as our team searched about investigation of the inhibition effect of *Althermanthera* and *Cionuraerecta* (L.) Griseb extracts. In the present study, the *Amaranthus*, *Althermanthera*, and *Cionuraerecta* (L.) Griseb extracts are applied for the first time as eco-friendly and cost-effective corrosion inhibitor sources for mild steel in the solution of 0.5 mol L^{-1} HCl. EIS and polarization tests were employed to investigate the corrosion inhibition effectivity of nanoemulsions and the extracts' corrosion inhibition mechanism on mild steel surfaces in an HCl solution. SEM was used for surface studies and the cytotoxicity impact of different concentrations of extracts on A172 and SHSY5Y cell lines was evaluated by using an MTT assay.

Experimental

Materials

The concentrated acid solutions (HCl), supplied by Merck Co. and were used with no further purifying treatment. Fetal bovine serum (FBS) and Dulbecco's modified Eagle medium (DMEM) were provided from Gibco BRL (America). Dimethyl sulfoxide (DMSO) and 3-(4,5-dimethylthiazol-2-yl)-2,5-diphenyl tetrazolium bromide (MTT) were obtained from Sigma (America). Figure 1 shows the herbal drugs' image. Working electrodes (WEs) with the surface area of 1 mm^2 from mild steel were prepared. The mild steel chemical composition contained (wt%): C (0.15), Mn (0.73), Si (0.72) and Fe (balance).

A B C

Figure 1. Herbal drugs images A: *Amaranthus*, B: *Althermanthera*, C: *Cionuraerecta* (L.)

Extraction of herbal plants and their nano-emulsification

Extraction of essential oils

Microwave oven equipped with Clevenger-type device of Tecnokit Chen (Italy, Tek- 2611) model, consisting of a multimode microwave reactor with a maximum delivered the power of 900 W, was used to perform Microwave Hydro-distillation. Leaves of Zataria multiflora were heated in 300 ml of water for 20 min. To obtain a high-quality essential oil, the plants' leaves were cleaned and rinsed with water ahead of each experiment and then underwent the extraction process until no more essential oil could be obtained. Finally, the essential oils were collected and stored in laboratory conditions.

Preparation of nanoemulsions

A solution of 2.0 wt% of SDS using double-distilled water was prepared at ambient conditions and stirred uniformly for 5min to reach a homogeneous solution state. Subsequently, 5.0 wt% of extracts were added gently to the prepared solution and stirred for 15 min using a magnet stirrer (Fine TECH, SDS-41; South Korea). Then a 25 kHz ultrasonic homogenizer (USH650, max power: 650W) was used to sonicate the obtained crude emulsion for a fixed amount of 20 min during all cases. Ultrasonication can generate solid and disruptive forces to reduce nanoemulsion droplets. Nanoemulsions were kept in laboratory condition.

Particle size measurements

To measure the nanoemulsion droplets' mean size (Z-averages), a dynamic light scattering device (DLS, model MAL1008078, Malvern, UK) was used. Such instruments can determine the particle size using the intensity-time fluctuations of laser beams (633 nm) emitted at an angle of 173° from the specimen. The measurements were averagely repeated for 1o times. To prevent the multiple scattering impacts, the samples were diluted with five mM, phosphate buffer (pH 7.4).

Methods

Corrosion studies (dynamic polarization and electrochemistry impedance)

In this study, the corrosion inhibition effect of the *Amaranthus, Althermanthera,* and *Cionuraerecta* (L.) Griseb nano-emulsion extracts impact on the steel surface layer immersed in 1 M HCl solution was evaluated by using the electrochemical i polarization method (Em State potentiostat galvanostat).

To perform the experiments, a conventional 3-electrode cell was used containing a metal electrode of size 1 × 1 cm (working electrode, WE), a larger area of Platinum mesh (counter

electrode, CE), and a saturated calomel electrode (reference electrode, RE). 25 ml of 1 M HCl solution without and with 30, 45, 70 and 100 mgL of plant extract was used for the experimental tests at differing temperatures (25, 40, 50 and 60 °C), and the related measurements were performed at open circuit potential (OCP) afterward 2 hours of immersion where the electrode was in its stable condition. As for measuring the potentiodynamic, the direction of cathodic direction the anodic was used at voltage ± 250 mV around OCP and a scan rate of 1.0 mVs.

Cell culture and treatment of cells by prepared nano-emulsion solutions

The researchers cultured the A172 and SH-SY5y cell lines as was reported above [30]. Cell biology science knows A172 as Man body basic glioblastoma cell line having epithelial morphology. To clone the SH-SY5Y, a biopsy derived bone marrow line designated as SK-N-SH was used, having been firstly published in the year 1973 [31]. A neuroblast-resembled subclone of SK-N-SH, called as SH-SY was subcloned as SH-SY5, again subcloned for the third round to obtain the SH-SY5Y line, firstly explained in 1978 [32].

The cloning process is primarily an artificial method of selection, comprising the expansion of a separate or small group of cells representing particular desired phenotypes, in this specific instance, neuron-resembled characteristics. The SH-SY5Y line, as genetically-known female, has two (2) X chromosome and no Y chromosomes. In summary, human cells are taken from A172 and SH-SY5Y lines (supplied by Pasteur Inst. of Iran, Tehran) were carefully cultured inside 25 cm^2 flasks (Iwaki, Tokyo, Japan) at 4 $\times 10^4$ cells/ml cell density in Dulbecco's Eagle medium (DMEM; Invitrogen Co. Gibco BRL, Gaithersburg, MD, USA). Then the cultured samples were supplemented by 10% (vv) inactivated serum of fetal calf plus 1% (vv) penicillin-streptomycin, then were kept in a humidified condition of 5% CO_2 at 37 ± 0.5 °C. The used medium was subsequently was replaced daily. Cell groups comprising 4 $\times 10^4$ cells (for the individual cell line) were examined for 24 and 48 hours, while categorized into four groups: 1) no treatment, 2) group treated at various concentrations (50–500 μgml) of MNPs, 3) group exposed to 100 Hz, 60±15 G MMF, and 4) a combined group of the MNPs and FMF treated cells. It is noteworthy that $NiFe_2O_4$ MNPs underwent suspension in DMEM medium, and nanocrystal suspensions underwent sonication for about 10 min at 40 W so to prevent agglomeration before treating the cells. Afterwards, each treatment, the morphological and biochemical examinations were also performed.

Cell viability

Decreased due to the active mitochondria present in the live cells [33]. The MTT tryout was carried out based on the modified method proposed by Sladowski et al. [34]. In short, 2×10^2 cells incubation was performed in 96-well plates (Iwaki) with 1 mgml of MTT in DMEM at 37 °C and 5% CO_2 for 2 hours. The cells subsequently were rinsed 3 times using 0.2-M phosphate buffer saline (PBS) (pH 7.4), and as for the stabilization of reduced MTT formazan crystals, they were put in 250 ml of DMSO. Next the optic density (OD) was recorded at 570 nm via an enzyme-linked immunosorbent test (ELISA) reader (Pharmacia Biotech, Stockholm, Sweden).

Statistical analysis

SPSS v16 (IBM, Armonk, NY, USA) was used for data analysis. Data were introduced to the software as mean standard error of the mean (SEM). To determine the significance among the treated versus control groups, t-Student's test at 95% confidence was used and P-values below 0.05 identified as significant.

Results and discussion

Nano-emulsion studies

By measuring the size of particles from the DLS strategy of nanosizer estimation, we prepared the particle size distribution curves. Figure 2 represents the synthesized sample sizes obtained from the DLS nanosizer. The samples of *Amaranthus, Althermanthea,* and *Cionuraerecta* (L.) Griseb show mean hydrodynamic sizes of 390 nm, 436 nm and 461 nm, respectively, showing that *Amaranthus* nano-emulsion represents the smallest size.

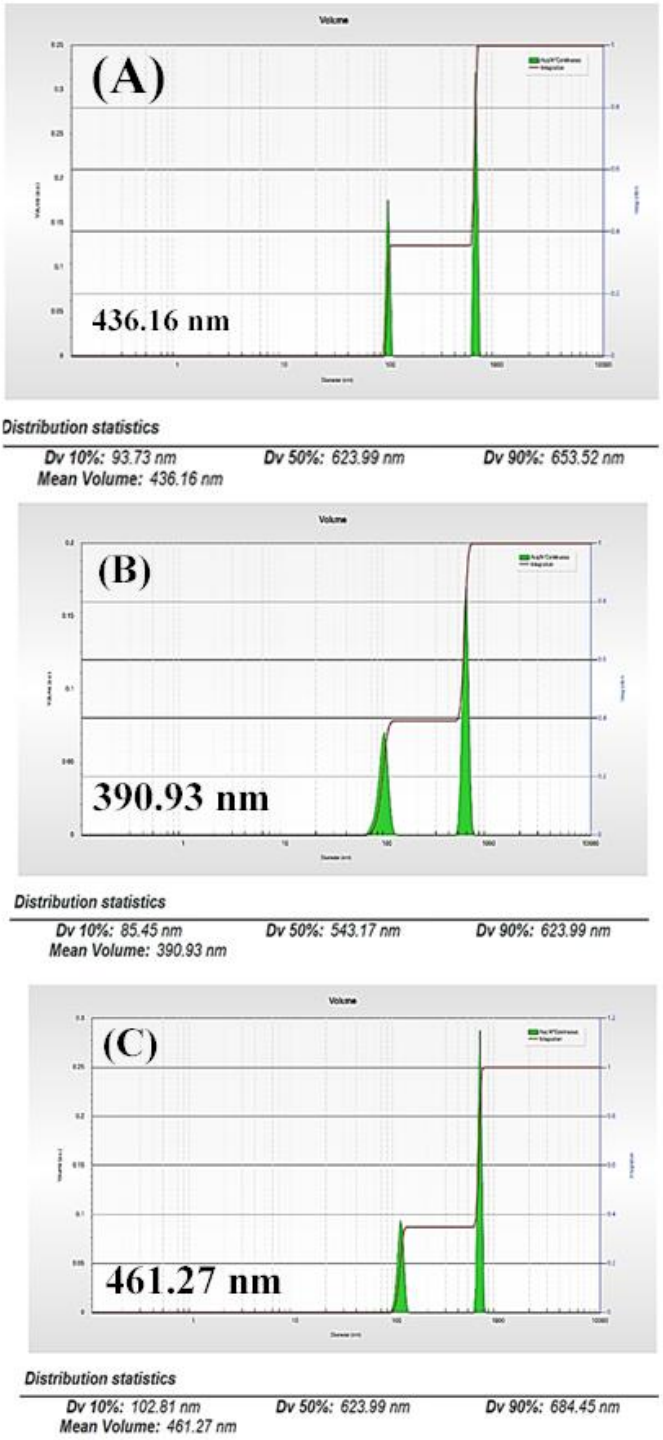

Figure 2. The synthesized samples size determined by DLS nanosizer.A: *Amaranthus*, B: *Althermanthera*, C: *Cionuraerecta*.

Potentiodynamic polarization

The curves illustrated in Figure 3 show the potentiodynamic polarization of mild steel immersed in 1.0 M HCl solutions in the absence and presence of differing concentrations of various nano-emulsion extracts. It is evident from the above figure that a typical Tafel behavior can be observed from the cathodic branch. As we will see later, this facilitates making the precise assessment of the cathodic Tafel slope and the corrosion currents (j_{corr}) through the Tafel extrapolation method. This is while the anodic polarization curve refrains from demonstrating the log-linear Tafel expected behavior across the potentials of the specified range.

The anodic branch, curvature could be associated with the deposition of corroded products like Fe3C and impurities on the steel, ending in the formation of non-passive surface films. Thus, because of the lack of linearity in the anodic branch, it would be impracticable to achieve the precise assessment of the anodic Tafel slope through Tafel extrapolation of the anodic branch. Investigations show that concerning the Tafel extrapolation technique, applying anodic and cathodic Tafel areas together is preferred over the application of only one Tafel area without doubt [35]. But the corrosion rate may also be specified via Tafel extrapolation of just the anodic or cathodic polarization curve. the case of employing only a single polarization curve, it is generally the cathodic curve which often generates a larger and suitably defined Tafel area (just as the point in this study). As for computing, the anodic current density obtained from the experiments, the Tafel line of the cathodic polarization curve initially was adjusted to zero overvoltage, and after that the equation below [35] was applied to determine the anodic current density:

where the a and c subscripts represent the anodic and cathodic directions respectively. Hence, the anodic current density equals the sum of recorded anodic current density plus the density of extrapolated cathodic current. Table (1-3) lists the relevant parameters such as corrosion potential (Ecorr), corrosion current density (icorr), and cathodic- anodic Tafel slopes (a, _c). Findings showed that the current density of corrosion was reduced by the increase in inhibitor concentration up to 100 mg/L. Adding extracts to acidic media influenced both the anodic and cathodic branches of the potentiodynamic polarization curves. Accordingly, the extracts showed a mixed inhibitor behavior. The above tables also present the efficiency values resulting from corrosion inhibition (IE), for the calculation of which the below expression could be used [36]:

where icorr and icorr represent the densities of corrosion current throughout no-inhibition and inhibition cases respectively. Increasing the concentration of inhibitor to 100 mg/L escalated

the IE values. Such findings are also indicative of inhibitor properties of *Amaranthus*. The experimental results show that any inhibitor concentration increase would cause a reduction of current density value (i_corr) as well as a relevant increase in the IE value, attributable to the rise in the coverage of surface (90%) by the inhibitor, resulting in the equation of IE100 [37].

Figure 3 represents the cathodic and anodic polarization curves relative to the steel dipped in 0.5 M HCl solution in the absence and presence of plant extract with various concentrations (30, 45,70 and 100 mgL). The polarization plots show numerous parameters with electrochemical properties such as corrosion current density (Icorr), corrosion potential (Ecorr), corrosion rate (C.R), inhibition efficiency (IE %) and cathodic Tafel slope (βc). The relevant results are contained in Tables (1–3). Notably, there was not any linear Tafel area in the curves' anodic branches. Therefore, the anodic Tafel slope values (ßa) and especially the current densities (Icorr) of corrosion are impossible to determine through the interpolation technique. To provide a solution to this problem, we introduced the cathodic asymptote interpolation with a line crossing the Ecorr denoting the corrosion current density.

As shown from Figure 3a, the addition of *Amaranthus* with an even lower concentration to 0.5 M HCl solution generated a change of cathodic and anodic branches towards lower current densities and minimal shift to less negative values about to the corrosion potential. The results are showing that the thickness of corrosion current would decrease and the inhibitor performance would increase with the increase in the concentration of *Amaranthus*. V increase in *Amaranthus* concentration led to the significant reduction of cathodic Tafel slope and a little addition of corrosion probability towards slighter negative figures. The results also show that *Amaranthus* influenced the anodic branch shape greater than the cathodic branch. Thus, the findings above demonstrate that *Amaranthus* behaved like a mixture-type inhibitor producing a dominant impact on anodic reactional activities. The findings of the experiment carried out on the steel in 0.5 M HCl solutions with and without *Althermanthera* plant extract and *Cionuraerecta*(L.) resulted in the same behavior. As can be noticed from Tables 1-3, a corrosion rate increasing trend, as well as corrosion current density accompanied by a decreasing trend for the effectiveness of corrosion inhibition may be observed due to the increase in the extracts' concentration [38,39]. The adsorption mechanism acts based on the Langmuir adsorption isotherm. The adsorption free energy value showed that *A: Amaranthus, B: Althermanthera, C: Cionura erecta (L.)* extracts will

lead to physical adsorption (Table 4) compared with the nanoemulsion that would be indicative of the physical-chemical adsorption.

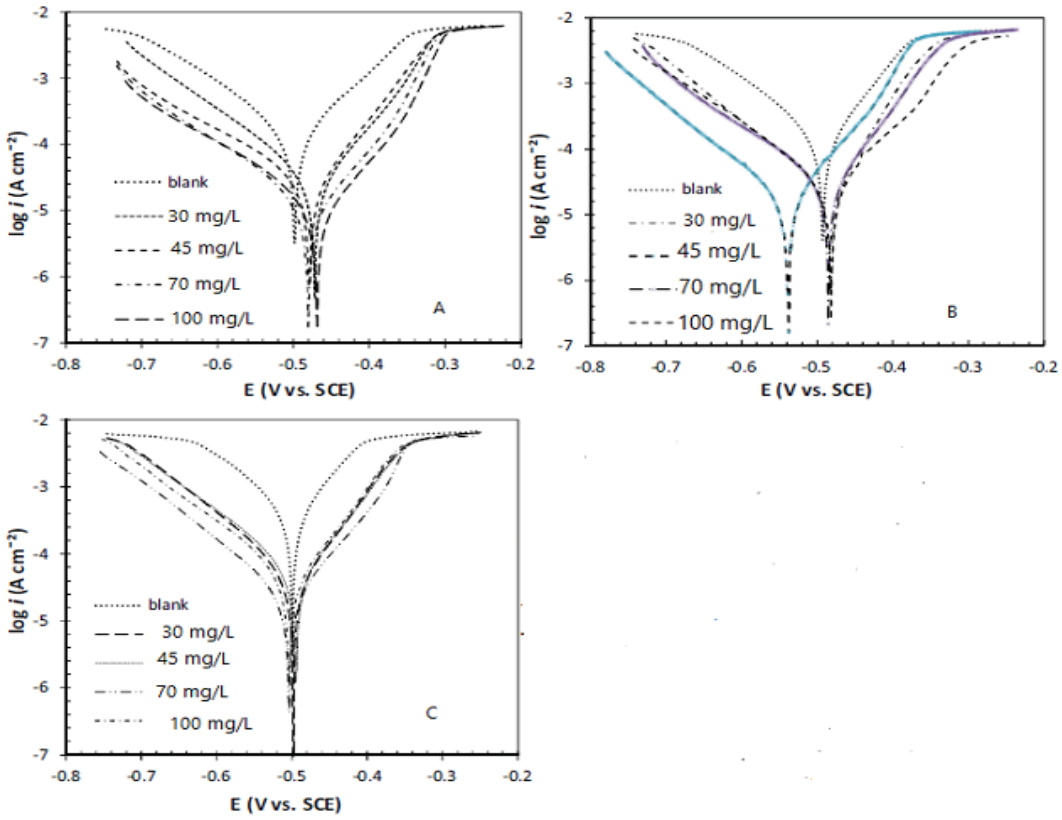

Figure 3. polarization plot A: *Amaranthus* , B: *Althermanthera* , C: *Cionuraerecta.*

Table 1. Electrochemical parameters of *Amaranthus.*

C(mg/L)	E (mV)	$-\beta_c$	Icorr (µA/cm2)	CR (mpy)	IE%
0	-496.7	50.5	155	2.36	-
30	-470.6	10.2	31	0.47	78
45	-478.5	22.5	25	0.40	81
70	-478.5	18.5	12	0.19	90
100	-470.9	6.4	10	0.13	91

Table 2. Electrochemical parameters of *Althermanthera*

C(mg/L)	E (mV)	$-\beta_c$	Icorr (µA/cm2)	CR (mpy)	IE%
0	-498.7	55.5	153	2.26	-
30	-570.6	25.2	36	1.35	78

45	-488.5	21.5	28	0.38	81
70	-478.5	15.5	17	0.17	83
100	-470.9	5.4	13	0.12	82

Table 3. Electrochemical parameters of *Cionuraerecta* (L.).

C(mg/L)	E (mV)	$-\beta_c$	Icorr (µA/cm2)	CR (mpy)	IE%
0	-499.7	7.8	268	2.9	-
30	-496.6	9.2	64	0.69	75
45	-498.5	12.3	59	0.62	78
70	-507.5	16.9	45	0.18	85
100	-507.9	17.1	42	0.10	83

Table 4. thermodynamic data of A: *Amaranthus* , B: *Althermanthera* , C: *Cionuraerecta* adsorption on mild steel.

Compound	R^2	Slope	Intercept(g/I)	K(I/g)	ΔG(kJ/mol)
A: *Amaranthus*	0.998	1.048	0.00393	254.5	-24.7
B: *Althermanthera*	0.997	1.101	0.000025	4000	-30.5
C: *Cionuraerecta*	0.997	1.176	0.00046	2175	-28.9

Surface studies

The SEM analysis was employed to examine the extracts' effect on the surface morphology of the steel after immersion into HCl electrolyte. The SEM images are shown in Figure 4 indicated that all extracts in 100 mg/L concentration made the steel surface smoother with some damage and corroded areas. So, it can be said that the adsorption of extracts' molecules by the corrosion sites residing on the metal substrate caused a reduced surface roughness due to its metal corrosion mitigation property [40-44].

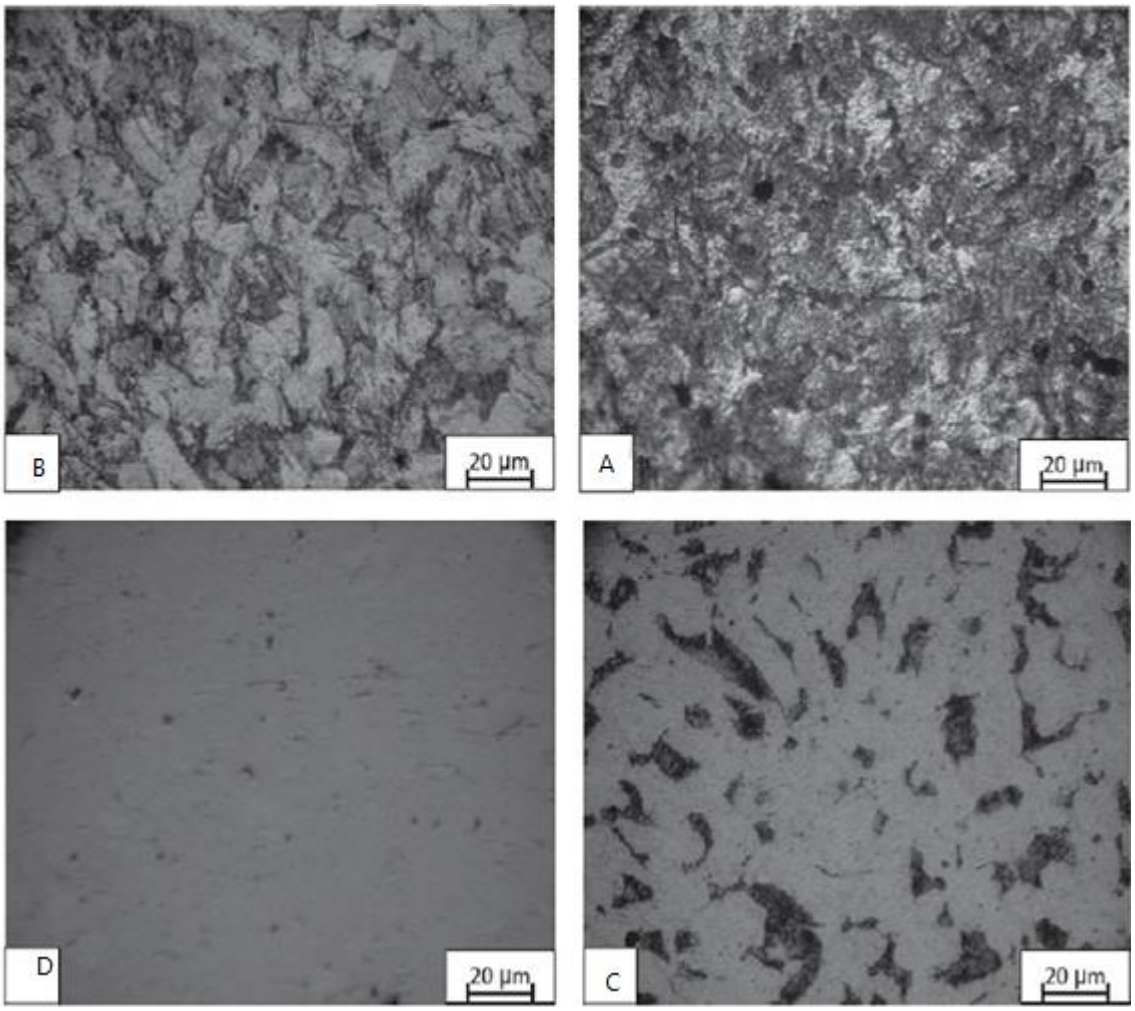

Figure 4. SEM of surface. A: without inhibitor B: by adding *Amaranthus*, C: by adding *Althermanthera*, D: by adding *Cionuraerecta* (L.).

Cytotoxicity

MTT cytotoxicity test was carried out on the A172 and SHSY5Y cell lines (of human primary glioblastoma and neuroblastoma cell line) and the pertaining cell viability was illustrated in Figures 5-10. The cells were seeded at a10×10^3 number of cells per good density in well plates (96) and kept in a CO_2 incubator at temp. 37 °C for 24 hours. Afterwards, different concentrations of extracts suspension were added to every cell individually and incubated for another 24 h. The concentrations ranged from 1 to 16 mgml. The media content was refreshed and an addition of 10µL MTT (5%) filtered solution was made to every cell and then incubated for 2 hours. The researchers used the following formula to record the cell viability [45]:

$$\text{Cell viability percentage} = (A_{test}\ A_{ctrl}) \times 100$$

where A_{test} and A_{ctrl} represent the test absorbance values and the control cell respectively, As evident from the figures, serious extracts' toxicity (>80% cell viability) was recorded with lower concentrations (˷2 mgmL), indicating the acceptable anticancer activity of the specimens. A growth of inhibition at higher concentrations however was investigated, revealing that the extracts show concentration-based toxicity behavior toward cells. Also, the high cell viability of *Cionuraerecta* (L.) extract relative to A-172 cell lines compared to Shsy5y cells in all concentrations can be attributed to the selectivity of this extract.

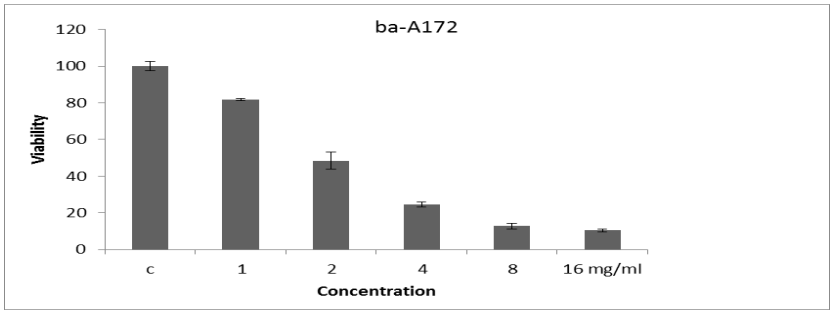

Figure 5. MTT assay of *Amaranthus* on A172 cell lines.

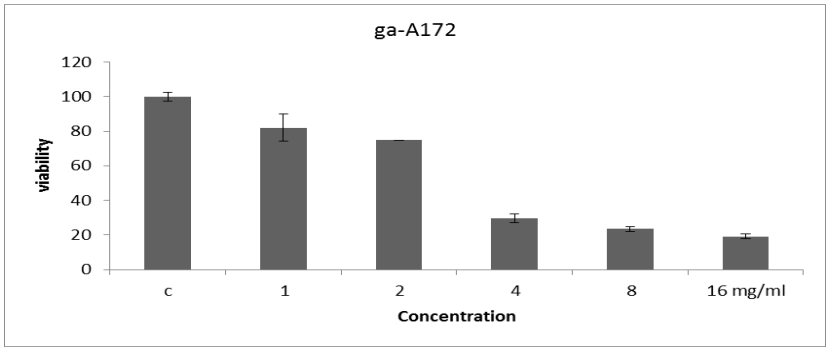

Figure 6. MTT assay of *Althermanthera* on A172 cell lines.

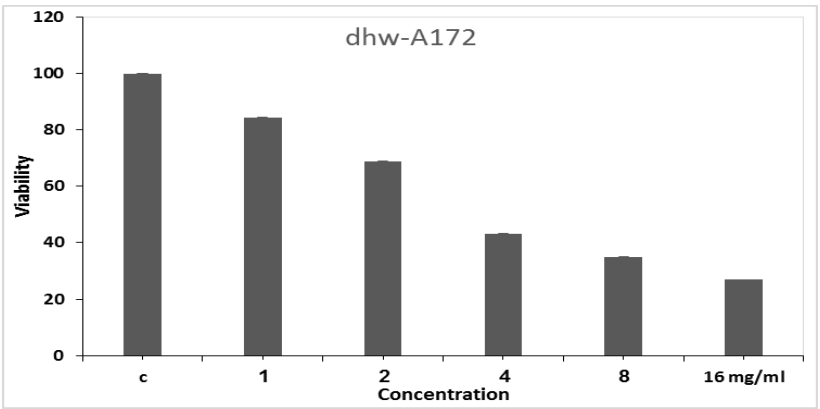

Figure 7. MTT assay of *Cionuraerecta* (L.)on A172 cell lines.

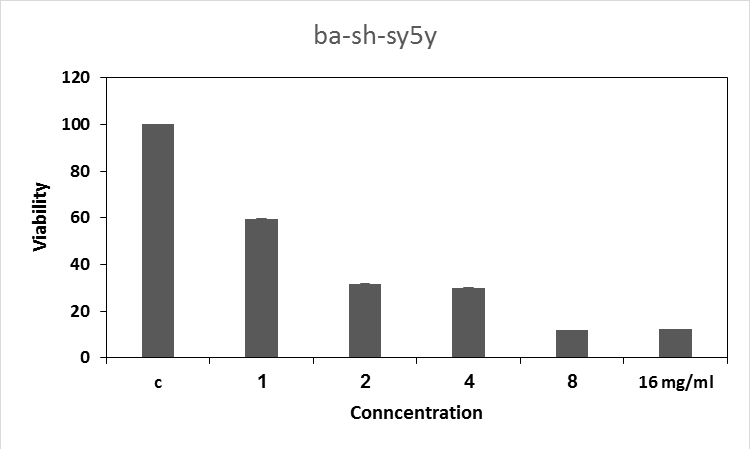

Figure 8. MTT assay of Amaranthus on sh-sy5y cell lines.

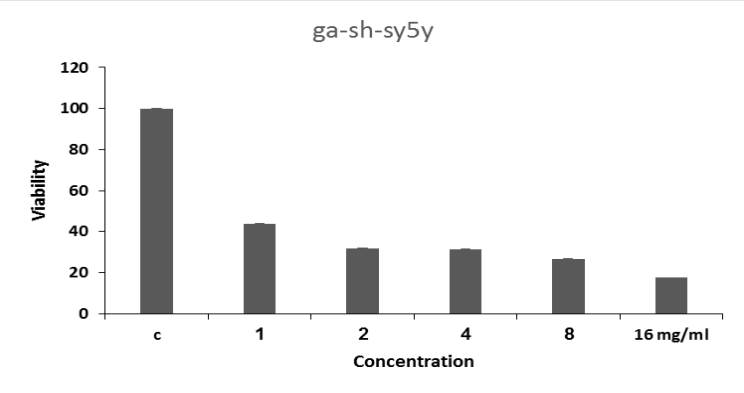

Figure 9. MTT assay of Althermanthera on sh-sy5y cell lines.

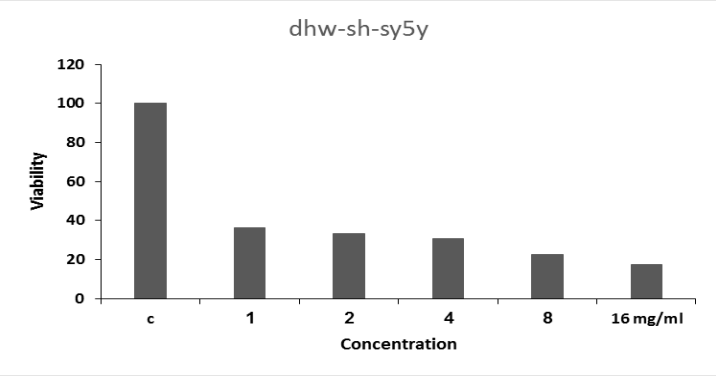

Figure 10. MTT assay of Cionuraerecta (L.) on A172sh-sy5y cell lines.

Conclusion

The present paper introduced a nano-emulsion strategy to enhance the corrosion inhibition efficacy of various herbal extracts for mild steel in acidic environments. Weight loss, dynamic polarization, and electrochemical impedance spectroscopy presented that the inhibitor ability increases with the nano-emulsion samples concentration increase. The

proposed method yielded 91% inhibitor efficiency in the presence of 100 mg/L of the nano-emulsion *Amaranthus*. Adsorption mechanism confirmed via Langmuir adsorption isotherm. The calculated adsorption free energy value indicated physical adsorption. SEM surface images confirmed the corrosion inhibition of mild steel in the presence of herbal extracts. MTT test on A172 and SHSY5Y cell lines demonstrated the extracts' anticancer effect over all the concentration ranges applied.

References

[1]C. Verma, L.O. Olasunkanmi, E.E. Ebenso, M.A. Quraishi, I.B. Obot,*J. Phys. Chem. C.*, 120, 11598(2016).

[2]P. Singh, E.E. Ebenso, L.O. Olasunkanmi, I.B. Obot, M.A. Quraishi, *J. Phys. Chem.C.*, 120, 3408(2016).

[3]S. M. A. Hosseini, M. Amiri, A. Momeni, *Sur Rev and Let.*,15, 435(2008) .

[4]C. Verma, H. Lgaz, D.K. Verma, E.E. Ebenso, I. Bahadur, M.A. Quraishi, *J. Mol. Liq.*, 260 , 99(2018).

[5]K. Zhang, W. Yang, X. Yin, Y. Chen, Y. Liu, J. Le, B. Xu, *Carbohydr.Polym.*, 181, 191(2018).

[6]C. Verma, J. Haque, E.E. Ebenso, M. Quraishi, *Results in Physics*, 9, 100 (2018).

[7]C. Verma, M. Quraishi, E.E. Ebenso, I. Bahadur, *J Bio-and Tribo-Corr.*,4, 33(2018).

[8]C. Verma, L.O. Olasunkanmi, T.W. Quadri, E.-S.M. Sherif, E.E. Ebenso, *J. Phys. Chem. C.*, 122, 11870(2018).

[9] C. Verma, E.E. Ebenso, M.A. Quraishi, Green Chem., InTech 2018.

[10]S. Nofrizal, A.A. Rahim, B. Saad, P.B. Raja, A.M. Shah, S. Yahya, *Metall. Mater. Trans. A.*, 43, 1382(2012).

[11]R. Ahmad, A. Mirza, *J. Mol. Liq.*, 249, 805(2018).

[12]C. Verma, E.E. Ebenso, M.A. Quraishi, *J. Mol. Liq.*, 233, 403(2017).

[13]C. Verma, L.O. Olasunkanmi, E.E. Ebenso, M.A. Quraishi, *J. Mol. Liq.*, 251, 100(2018).

[14]C. Verma, E.E. Ebenso, M.A. Quraishi, *J. Mol. Liq.*,248, 927(2017).

[15] X. Zheng, M. Gong, Q. Li, L. Guo, *Scientific reports.*, 8,9140(2018).

[16] Z. Zhang, H. Ba, Z.Wu, *Constr. Build. Mater*., 227, 117080(2019).

[17] H. Hassannejad, A. Nouri, *J. Mol. Liq.*, 254, 377(2018).

[18] L.B.Molina-Ocampo, M.G. Valladares-Cisneros, J.G. Gonzalez-Rodriguez, *Int. J. Electrochem. Sci.*, 10,388(2015).

[19] P. Parthipan, J. Narenkumar, P. Elumalai, P.S. Preethi, A.U.R. Nanthini, A. Agrawal, A. Rajasekar, *J. Mol. Liq*., 240,121(2017).

[20] S. Varvara, R. Bostan, O. Bobis, L. Găină, F. Popa, Vi. Mena, R.M. Souto, *Appl. Surf. Sci.*, 426,1100(2017).

[21] M.M. Fares, A.K.Maayta,M.M. Al-Qudah, *Corr. Sci.*, 60, 112(2012).

[22] P. Mourya, S. Banerjee, M.M. Singh, *Corr. Sci.*, 85,352(2014).

[23] A. Ostovari, S.M. Hoseinieh,M. Peikari, S.R. Shadizadeh, S.J. Hashemi, *Corr. Sci*., 51, 1935(2009).

[24] G. Ji, S. Anjum, S. Sundaram, R. Prakash, *Corr. Sci*., 90, 107(2015).

[25] N. Asadi, M. Ramezanzadeh, G. Bahlakeh, B. Ramezanzadeh, *J. Taiwan Inst. Chem. E.*, 95, 252(2019).

[26] M. Ramezanzadeh, G. Bahlakeh, Z. Sanaei, B. Ramezanzadeh, *Appl. Surf. Sci.*, 463, 1058(2019).

[27] B. Obot, S.A. Umoren, N.K. Ankah, *J. Mol. Liq*., 277, 749(2019).

[28] E. Alibakhshi, M. Ramezanzadeh, G. Bahlakeh, B. Ramezanzadeh, M. Mahdavian, M. Motamedi, *J. Mol. Liq*., 255, 185(2018).

[29] L.B. Furtado, R.C. Nascimento, P.R. Seidl, M.J.O.C. Guimaraes, L.M. Costa, J.C. Rocha, *J. Mol. Liq.*, 284, 393(2019).

[30] M. Amiri, A. Akbari, M. Ahmadi, A. Pardakhti, M. Salavati-Niasari, *J. Mol. Liq*.,249, 1151(2018).

[31] J.L. Biedler, L. Helson, B.A. Spengler, *Cancer Res.*, 33, 2643(1973).

[32] J.L. Biedler, S. Roffler-Tarlov, M. Schachner, L.S. Freedman, *Cancer Res.*, 38, 3751(1978).

[33] T. Mosmann, *J. Immunol. Methods.*, 65, 55(1983).

[34] D. Sladowski, S.J. Steer, R.H. Clothier, M. Balls, , *J. Immunol. Methods.*, 157, 203(1993).

[35] M. Banu, R. Joany, S. Rajendran, *Der PharmaChemica.*, 10, 123 (2018).

[36]M. Mobin, M. Rizvi, *Carbohydr. Polym*., 160, 172(2017).

[37]H. Bourazmi, M. Tabyaoui, L. Hattabi, Y. El Aoufir, M. Taleb, ,*J Mater. and EnvironSci.,* 9, 928(2018).

[38] Shweta Pal, Hassane Lgaz, Preeti Tiwari, Ill-Min Chung, Gopal Ji, Rajiv Prakash, *J. Mol. Liq.,* 276, 347(2019).

[39] Ghasem Bahlakeh , Bahram Ramezanzadeh , Ali Dehghani , Mohammad Ramezanzadeh , *J. Mol. Liq*., 283, 174(2019).

[40]K. Anupama, A. Joseph, *Jo Bio-and Tribo-Corr*., 4,1(2018).

[41]J. Stephen, A. Adebayo, *J. Fail. Anal. Prev*., 18, 350(2018).

[42]A. Saxena, D. Prasad, R. Haldhar, *J.Fail. Anal. Prev*., 18, 957(2018).

[43]E. Alibakhshi, M. Ramezanzadeh, S.A. Haddadi, G. Bahlakeh, B. Ramezanzadeh, M.Mahdavian, *J. Clean. Prod*., 210, 660(2019).

[44]E. Alibakhshi, M. Ramezanzadeh, G. Bahlakeh, B. Ramezanzadeh, M. Mahdavian, M.Motamedi, *J. Mol. Liq*., 255, 185(2018).

[45]R.S. Mayanglambam, V. Sharma, G. Singh, *Port. Electrochim.Acta.*, 29, 405(2011).